A scanning tunneling microscopy study of atomic-scale clustering in InAsP/InP heterostructures

S. L. Zuo, W. G. Bi,[a] C. W. Tu, and E. T. Yu[b]
Department of Electrical and Computer Engineering, University of California, San Diego, La Jolla, California 92093-0407

(Received 16 February 1998; accepted for publication 26 February 1998)

We have used cross-sectional scanning tunneling microscopy to perform atomic-scale characterization of $InAs_{0.35}P_{0.65}$/InP strained-layer multiple-quantum-well structures grown by gas-source molecular-beam epitaxy. High-resolution (110) cross-sectional images reveal nanoscale clustering of As and P in the $InAs_xP_{1-x}$ alloy layers. Boundaries between As-rich and P-rich regions in the alloy layers appear to be preferentially oriented along the [112] and [$\bar{1}$12] directions in the (110) plane, suggesting that boundaries between As-rich and P-rich clusters tend to form within {111} planes in the lattice. The nanoscale compositional variations within the $InAs_xP_{1-x}$ alloy layers lead to an asymmetry in interface quality in the (110) cross section, with the $InAs_xP_{1-x}$-on-InP interfaces being much smoother and more abrupt than the InP-on-$InAs_xP_{1-x}$ interfaces. Analysis of (110) cross-sectional images suggests that the clusters formed within the $InAs_xP_{1-x}$ alloy are elongated along the [110] direction in the crystal. © *1998 American Institute of Physics.* [S0003-6951(98)02317-1]

$InAs_xP_{1-x}$/InP heterostructures have shown considerable promise for optoelectronic devices such as lasers[1–4] and photodetectors[5] operating at 1.06–1.55 μm, and for high-speed electronic devices.[6] In quantum-well laser structures, compressive strain in the $InAs_xP_{1-x}$ layer leads to a smaller valence-band effective mass and, consequently, a smaller valence-band density of states that facilitates population inversion.[7] Furthermore, the large conduction-band offset in this material system[8] ($\Delta E_c \cong 0.75 \Delta E_g$) leads to efficient electron confinement and reduced leakage current in laser diodes, thereby minimizing the threshold current in $InAs_xP_{1-x}$/InP lasers.[1] Finally, compositions in the $InAs_xP_{1-x}$/InP system are easier to control than those in the $In_xGa_{1-x}As_yP_{1-y}$/InP system, which has also been explored extensively for optoelectronic device applications at wavelengths of 0.98–1.55 μm.[3,9]

A significant issue in ternary and quaternary III–V alloys is the possible presence of ordering, clustering, and/or compositional modulation phenomena, which have been observed to occur in a wide range of material systems[10–12] and which can exert a considerable influence on crystal quality, interface quality, and other electronic as well as optical properties such as band gap,[13] band-edge discontinuities, and carrier transport.[14–17] Detailed characterization and understanding of these phenomena at the atomic scale are, therefore, of great importance for optoelectronic and electronic devices based on these materials.

In this letter, we describe cross-sectional scanning tunneling microscopy (STM) studies of atomic-scale compositional structure in an $InAs_{0.35}P_{0.65}$/InP strained-layer multiple-quantum-well (MQW) structure grown by gas-source molecular-beam epitaxy (MBE) on n^+-InP (001) substrates. The epitaxial-layer structure of the samples used in these studies and the cross-sectional STM geometry employed are illustrated schematically in Fig. 1. A 2500 Å InP buffer layer was grown initially, followed by a coherently strained heterostructure consisting of 50 Å $InAs_{0.35}P_{0.65}$ alternating with 100 Å InP for five periods. All epitaxially grown layers were doped n type ($n \sim 10^{16}$–10^{17} cm^{-3}). The substrate temperature during growth was 460 °C; further details concerning the growth chamber and procedures are described elsewhere.[18,19] STM studies were performed on both (110) and ($\bar{1}$10) cross-sectional surfaces exposed by *in situ* cleaving in an ultra-high-vacuum STM chamber at a pressure

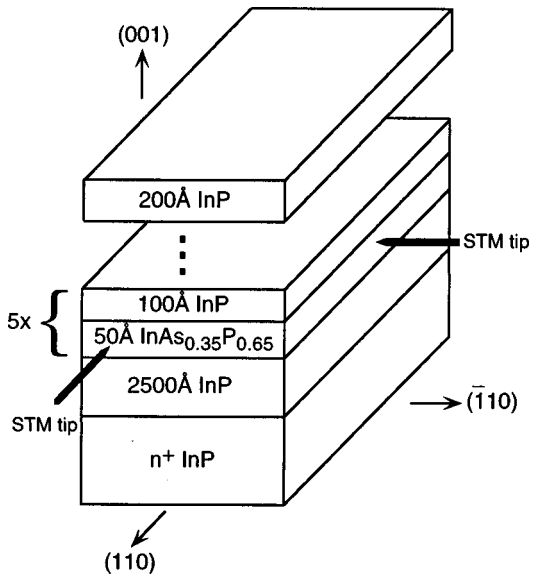

FIG. 1. Schematic diagram of the sample structure and STM geometry used in these studies. The epilayer consisted of a 2500 Å InP buffer layer grown on a (001) n^+-InP substrate, followed by a five-period, 50 Å $InAs_{0.35}P_{0.65}$/100 Å InP n-type multiple-quantum well. STM imaging was performed on both (110) and ($\bar{1}$10) cross-sectional planes.

[a]Present Address: Hewlett-Packard Company, 3500 Deer Creek Road, MS 26M-7, Palo Alto, CA 94304.
[b]Electronic mail: ety@ece.ucsd.edu

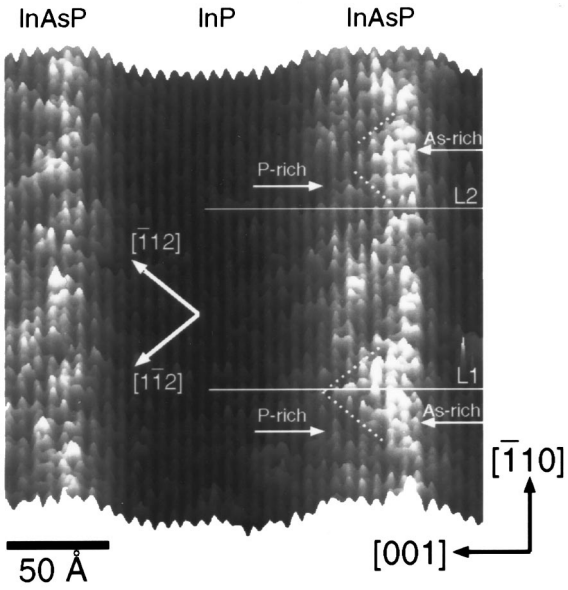

FIG. 2. Three-dimensional rendering of a 205 Å×205 Å (110) constant-current STM image of the $InAs_{0.35}P_{0.65}$/InP multiple-quantum-well structure, obtained at a sample bias voltage of −2.4 V and a tunneling current of 0.1 nA. Major directions are indicated by arrows. Two triangular As-rich regions, bounded by dotted lines, and two P-rich regions are indicated.

of $\sim(6-9)\times10^{-11}$ Torr. Electrochemically etched W tips, cleaned *in situ* by electron bombardment, were used for these studies.

Figure 2 shows a three-dimensional rendering of a 205 Å×205 Å (110) constant-current STM image of the $InAs_xP_{1-x}$/InP multiple-quantum-well structure, obtained at a sample bias of −2.4 V and a tunneling current of 0.1 nA. Because the valence-band edge of InAs is higher than that of InP, we interpret the brighter features as being associated with As atoms and the darker features with P within the $InAs_xP_{1-x}$ layer. Variations in composition at the atomic scale are clearly visible, allowing us to investigate in detail the nature of clustering in the $InAs_xP_{1-x}$ layer. From Fig. 2, it is apparent that there exist brighter As-rich clusters and darker P-rich clusters within the $InAs_xP_{1-x}$ alloy layer, as indicated by the labeled arrows. As a direct consequence of nanoscale clustering of As and P within the $InAs_xP_{1-x}$ alloy layers, there is a marked asymmetry in interface quality—the InP-on-$InAs_xP_{1-x}$ interfaces are considerably rougher and less abrupt than the $InAs_xP_{1-x}$-on-InP interfaces. Clustering of As and P in the $InAs_xP_{1-x}$ alloy layer can be further substantiated by examination of topographic line scans extracted from different regions in Fig. 2. Figure 3 shows topographic line scans, each averaged across one atomic spacing along the [110] direction, extracted from locations indicated in Fig. 2. The line scans L1 and L2 correspond to an As-rich region and a P-rich region, respectively, within the $InAs_xP_{1-x}$ alloy layer. Within the first five to six bilayers of the $InAs_xP_{1-x}$ alloy, the topographic profiles in the As-rich and P-rich regions differ substantially, reflecting a significant difference in composition. Near the top of the $InAs_xP_{1-x}$ layer, i.e., above the As-rich cluster traversed by L1, the topographic profiles are much more similar.

An additional feature observed in the $InAs_xP_{1-x}$ alloys is that the intersections in the (110) plane of the boundaries

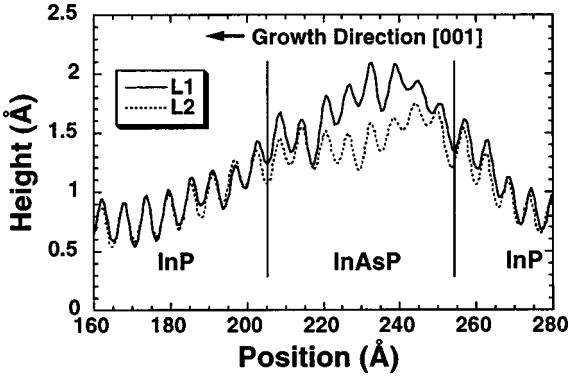

FIG. 3. Topographic line profiles L1 and L2 extracted from the As-rich and P-rich regions, respectively, of the $InAs_xP_{1-x}$ alloy indicated in Fig. 2.

between As-rich and P-rich regions appear to be preferentially oriented along the [112] and [112] directions. In Fig. 2, the dotted lines delineate two As-rich regions, each starting from the $InAs_xP_{1-x}$-on-InP interface and extending in the [001] growth direction for approximately 30–35 Å. These regions appear to be approximately triangular, with bases extending 40–60 Å in the [110] direction and sides oriented along the [112] and [112] directions. If the boundaries between As-rich and P-rich regions assume the form of simple planes, then we may deduce from the intersections of these boundaries with the (110) plane that their indices (hkl) should satisfy the equation

$$\mp(h-k)+2l=0. \tag{1}$$

The simplest solutions to Eq. (1) correspond to $(\bar{1}11)$ and (111) planes in the crystal, suggesting that the boundaries between As-rich regions and P-rich regions may form preferentially within these planes.

Further information about the nanoscale compositional structure of the $InAs_xP_{1-x}$ alloy layers can be obtained by analysis of cross-sectional images of the (110) plane. Figure 4(a) shows a three-dimensional rendering of a 400 Å ×400 Å (110) constant-current STM image of the $InAs_xP_{1-x}$/InP MQW structure, obtained at a sample bias of −2.4 V and a tunneling current of 0.1 nA. The $InAs_xP_{1-x}$ alloy layers show considerably less compositional variation along the [110] direction than was evident along the [110] direction in the (110) cross-sectional image. It is also apparent that the As composition is graded along the [001] growth direction within the two lower (i.e., right most in the image) $InAs_xP_{1-x}$ alloy layers: the topographic contrast in Fig. 4(a) is generally greater near the $InAs_xP_{1-x}$-on-InP interfaces than that near the InP-on-$InAs_xP_{1-x}$ interfaces, indicating that the As concentration is higher near the $InAs_xP_{1-x}$-on-InP interfaces and lower near the InP-on-$InAs_xP_{1-x}$ interfaces. Figure 4(b) shows three line scans, each averaged across one atomic spacing, extracted from the locations indicated by arrows in Fig. 4(a). Within the two lower $InAs_xP_{1-x}$ alloy layers, the topographic contrast decreases along the [001] growth direction, and the transition at the InP-on-$InAs_xP_{1-x}$ interface is much less abrupt than that at the $InAs_xP_{1-x}$-on-InP interface. Finally, the relatively uniform As composition observed along the [110] lateral direction in the (110) cross-sectional image combined with the triangular As-rich and P-rich clusters observed in the (110)

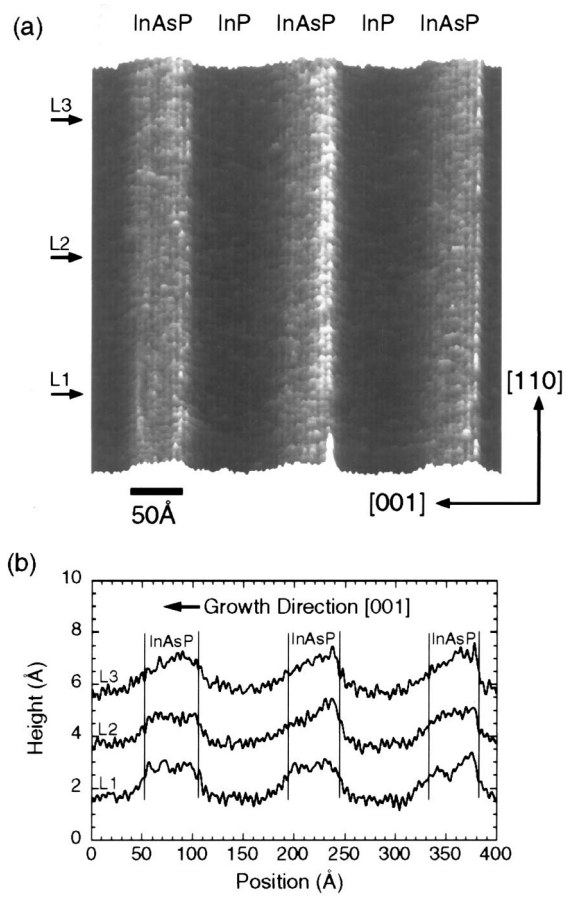

FIG. 4. (a) Three-dimensional rendering of a 400 Å×400 Å $(\bar{1}10)$ constant-current STM image of the $InAs_{0.35}P_{0.65}$/InP multiple-quantum-well structure, obtained at a sample bias voltage of −2.4 V and a tunneling current of 0.1 nA. (b) Topographic line profiles extracted from the locations indicated in (a), each averaged across one atomic site.

cross-sectional image suggests that the As-rich and P-rich clusters in the $InAs_xP_{1-x}$ alloy layers tend to be elongated along the [110] direction, with roughly triangular cross sections in the (110) plane.

In summary, we have performed atomically resolved cross-sectional STM imaging of $InAs_xP_{1-x}$/InP strained-layer multiple-quantum-well structures grown by gas-source MBE. These studies have revealed the presence of nanoscale clustering of As and P within the $InAs_xP_{1-x}$ alloy layers. Boundaries between As-rich and P-rich regions in the $InAs_xP_{1-x}$ alloy layers are oriented preferentially along the [112] and [112] directions in (110) cross-sectional images, forming As-rich regions with triangular cross sections in the (110) planes. This observation suggests that the boundaries between As-rich and P-rich regions in the $InAs_xP_{1-x}$ alloy layers are likely to be {111} planes. Clustering in the $InAs_xP_{1-x}$ alloy layers leads to a clear asymmetry in the interface structure in the (110) plane, with the $InAs_xP_{1-x}$-on-InP interfaces being much smoother than the InP-on-$InAs_xP_{1-x}$ interfaces. (110) cross-sectional images reveal a compositional gradient that is frequently, but not universally, present within the $InAs_xP_{1-x}$ alloy layers, with the As composition generally appearing to be higher near the $InAs_xP_{1-x}$-on-InP interfaces and lower near the InP-on-$InAs_xP_{1-x}$ interfaces. Combining the information obtained from both (110) and (110) images suggests that the As-rich and P-rich clusters in the $InAs_xP_{1-x}$ alloy layers tend to be elongated along the [110] direction, with roughly triangular (110) cross sections in the (110) plane.

Part of this work was supported by DARPA (Optoelectronics Technology Center) and NSF (ECS 95-07986). One of the authors (E.T.Y.) would like to acknowledge receipt of a Sloan Research Fellowship.

[1] T. Fukushima, A. Kasukawa, M. Iwase, T. Namegaya, and M. Shibata, IEEE Photonics Technol. Lett. **5**, 117 (1993).
[2] T. K. Woodward, T.-H. Chiu, and T. Sizer II, Appl. Phys. Lett. **60**, 2846 (1992).
[3] H. Q. Hou, A. N. Cheng, H. H. Wieder, W. S. C. Chang, and C. W. Tu, Appl. Phys. Lett. **63**, 1833 (1993).
[4] J. F. Carlin, A. V. Syrbu, C. A. Berseth, J. Behrend, A. Rudra, and E. Kapon, *1997 IEEE 9th International Conference on Indium Phosphide and Related Materials*, Cape Cod, MA, 11–15 May 1997, p. 563.
[5] D. S. Kim, S. R. Forrest, G. H. Olsen, M. J. Lange, R. U. Martinelli, and N. J. Di Giuseppe, IEEE Photonics Technol. Lett. **7**, 911 (1995).
[6] W.-P. Hong, J. R. Hayes, R. Bhat, P. S. D. Lin, C. Nguyen, H. P. Lee, D. Yang, and P. K. Bhattacharya, *Technical Digest/International Electron Devices Meeting*, Washington, DC, 8–11 December, 1991, p. 243.
[7] E. Yablonovitch and E. O. Kane, J. Lightwave Technol. **6**, 1292 (1988).
[8] M. Beaudoin, A. Bensaada, R. Leonelli, P. Desjardins, R. A. Masut, L. Isnard, A. Chennouf, and G. L'Espérance, Phys. Rev. B **53**, 1990 (1996).
[9] H. Q. Hou and C. W. Tu, J. Electron. Mater. **21**, 137 (1992).
[10] H. R. Jen, D. S. Cao, and G. B. Stringfellow, Appl. Phys. Lett. **54**, 1890 (1989).
[11] H. R. Jen, K. Y. Ma, and G. B. Stringfellow, Appl. Phys. Lett. **54**, 1154 (1989).
[12] Y.-E. Ihm, N. Otsuka, J. Klem, and H. Morkoç, Appl. Phys. Lett. **51**, 2013 (1987).
[13] K. A. Mäder and A. Zunger, Appl. Phys. Lett. **64**, 2882 (1994).
[14] G. B. Stringfellow and G. S. Chen, J. Vac. Sci. Technol. B **9**, 2182 (1991).
[15] A. Zunger and S. Mahajan, in *Handbook on Semiconductors*, Vol. 3B, *Materials, Properties and Preparation*, edited by S. Mahajan (North-Holland, Amsterdam, Netherlands, 1994), p. 1399.
[16] P. K. Bhattacharya and J. W. Ku, J. Appl. Phys. **58**, 1410 (1985).
[17] A. Gomyo, T. Suzuki, and S. Iijima, Phys. Rev. Lett. **60**, 2645 (1988).
[18] T. P. Chin, B. W. Liang, H. Q. Hou, M. C. Ho, C. E. Chang, and C. W. Tu, Appl. Phys. Lett. **58**, 254 (1991).
[19] H. Q. Hou and C. W. Tu, Appl. Phys. Lett. **60**, 1872 (1992).